Title:

Local inspection of refractive index and thickness of thick transparent layers using spectral reflectance measurements in coherence scanning interferometry

Authors and affiliations:

Rémy Claveau[a,b,*]   E-mail address: r.claveau@unistra.fr

Paul Montgomery[a]   E-mail address: paul.montgomery@unistra.fr

Manuel Flury[a,b]   E-mail address: manuel.flury@insa-strasbourg.fr

[a] Laboratoire des Sciences de l'Ingénieur, de l'Information et de l'Imagerie (ICube), UDS-CNRS UMR 7357, 23 rue du Loess, 67037 Strasbourg, France.

[b] Institut National des Sciences Appliquées de Strasbourg (INSA Strasbourg), 24 Boulevard de la Victoire, 67084 Strasbourg cedex, France

Corresponding author: Rémy Claveau

Phone number: 0668783253

Abstract:

For a long time, obtaining with a great accuracy the optical and morphological properties of a transparent sample without degrading the layer has been challenging. To achieve these expectations, contactless techniques are well suitable and brought optical methods to the forefront. Over recent years white light scanning interferometry has been increasingly used for studying and characterizing transparent materials with thicknesses ranging from a few hundred nanometers to several micrometers. Then, multiple techniques have been developed to retrieve the transparent layer properties from interferometric data. The more recent techniques, based on the use of an error

function which defines the best fit between the experimental and theoretical data, allow the determination of the properties of very thin films (< 1 μm). We show here that a similar method can be applied to thicker layers (> 1 μm) for simultaneously measuring their optical and morphological properties, provided that a crucial step is carefully considered during the data acquisition process. This enables the simultaneous measurements of both the thickness and the refractive index (dispersion) without any prior assumptions about one of the two parameters. We demonstrate the proposed method by accurate measurements on a few micrometers thick PMMA layer as well as on a SnO_2 layer, which is a much more dispersive sample.

Main text:

1. Introduction

The possibility of determining the optical and morphological properties of an unknown transparent sample without any information about its composition has always been an important challenge in a wide range of domains and in particular in that of materials. Coherence scanning interferometry is already a well-established method for measuring surface roughness and structure in 3D on different kinds of materials [1]. Indeed, this far field imaging method enables submicron spatial resolution and high speed non-destructive analysis of large sample areas [2]. As regards transparent materials, the use of white light-based interferometric techniques has been demonstrated for providing local information concerning the thickness or refractive index of the sample. The oldest

known method consists in recording the interference signal of the layer and then looking at the optical path separating the interferograms from the front and rear interfaces of the layer at a specific point [3]. The technique mentioned has nevertheless a major drawback since it becomes unusable for very thin films. The extremely low thickness leads to a single global signal corresponding to a mix between the fringes from the top and bottom surfaces and prevents the accurate separation of each envelope peak. To deal with this problem, innovative solutions have been developed based on the processing of interferometric data. These methods use the analysis of interference fringes in the spectral domain and combine experimental measurements with theoretical models in order to recover the thickness of the transparent thin film [4]. The idea is to bring the model (describing the interferometric spectral response of the layer) to converge towards the experimental data by optimizing the value of the parameter sought. The fitting model corresponds for most of the time to the phase [5] or magnitude [6] of the Fourier transform of the interference signal since they contain the information on both the thickness and index of the film. Work has been carried out to determine which of these parameters leads to the most sensitive measurement [7].

Usually, knowing either the thickness or the optical index, the two techniques presented enable one of the two previous parameters to be obtained since the optical path traveled by the light over one round trip within the layer is related to both. In consequence, it is necessary to know one of the two parameters in order to find the value of the other. Determining both at the same time and from the same measurement remains a challenge. Li et al. [8] have nevertheless demonstrated this possibility using the processing of the interferometric signal in the spectral domain and by measuring three thin materials with thicknesses ranging from 100 nm to 300 nm. The simultaneous measurement of the thickness and the dispersion constants (refractive index) was

validated by comparison with the results obtained from ellipsometry. From this work, we concluded that this spectral method was not necessarily only applicable to thin films but could also be applied to thicker samples provided that more precautions need to be taken during the acquisition process. Even though the technique mentioned first, which relies on the measurement of the distance separating the interferograms, could also be applied in the case of thick layers, it remains far less accurate compared to the proposed technique and does not allow the measurement of the thickness and the optical index independently from each other if one of them is unknown. Furthermore, it is obviously impossible to extract the dispersion of the material.

2. Theory

The method proposed here is based on the spectral analysis of the interference fringes and uses the magnitude of the signal Fourier transform (FT). Similarly to what has been performed in [4], the first step is to develop the model used to describe the theoretical spectral behavior of the transparent layer. In the case of very thin films, with a thickness lower than the coherence length of the source, the multiple reflections of the light within the layer have to be taken into account and the magnitude of the FT corresponds then to the well-known total reflection coefficient [9]. For thick layers with an optical thickness (product of the real thickness and the optical index) exceeding the coherence length of the source, being ~ 2 µm in our case, a new model must be established. Indeed, the 2nd order reflections, i.e. the light coming back from the sample after propagating more than one round trip in the layer, must not be considered because it possesses an optical path much higher than that being reflected only once. This light interferes for a different position of the sample and is then either attenuated by the coherence zone of the

interferometric system [10] or merely suppressed during the signal processing (windowing).

The theoretical development of the interference signal of a transparent layer, neglecting the 2nd order reflections, followed by a Fourier transform calculation, leads to the expression of the spectral reflectance of the layer that can be written as:

$$\left| R_{\text{mod}}\left(\lambda\right)\right| = r_{01}^2 + r_{12}^2 \left(1 - r_{01}^2\right)^2 + 2 r_{01} r_{12} \left(1 - r_{01}^2\right)$$
$$\cos\left(\frac{4\pi}{\lambda} en + \phi_{01} - \phi_{12}\right) \tag{1}$$

The spectral reflectance $|R_{\text{mod}}|$ denotes the model that will be used to recover the properties of the layer, with e and n which are respectively its thickness and refractive index. r_{ij} and ϕ_{ij} refer respectively to the magnitude and phase of the Fresnel reflection coefficient of the interface ij (01: air/layer, 12: layer/air). It can be noted that the previous expression assumes that no absorption occurs during the light propagation. This hypothesis is validated for the samples studied here. To compute the Fresnel coefficient, the complex refractive index of the silicon substrate is extracted from [11].

3. Experimental details

3.1. Optical set-up

The experimental optical set-up used to carry out the experiments is an adapted Leitz-Linnik interference microscope (Fig. 1).
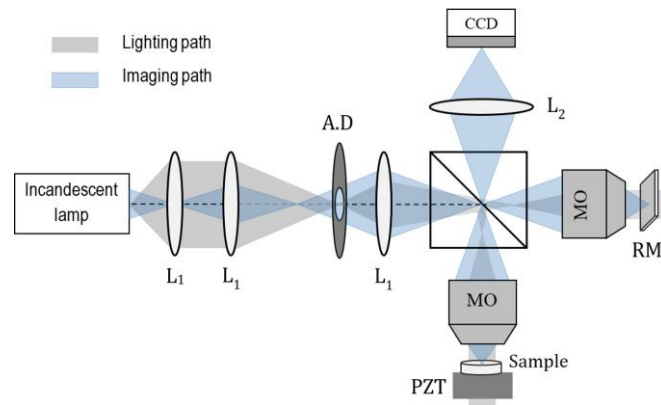
Fig. 1. Schematic diagram of the optical system. L1, aspheric lenses; L2, imaging lens f = 200 mm; A.D, aperture diaphragm; MO, 50x microscope objectives; RM, reference mirror; PZT, piezoelectric device for Z-scanning.

The source is an incandescent lamp with an 800 nm central wavelength and a 290 nm bandwidth. The illumination arm is built so as to obtain a Köhler illuminator providing a very homogeneous illumination of both the sample and the reference mirror. The aperture diaphragm enables the spatial coherence of the illumination to be controlled by adjusting the maximum angle of the incident light. After propagation of the light in both arms and reflection on the sample and the mirror, each reflected waves are focused onto the camera by the imaging lens. The resulting image is the superposition of the image of the sample, the image of the reference mirror and an interference pattern made of black and white fringes that depends on the difference of optical length between each arms. By scanning these fringes within the depth of the sample, one can obtain some information about the sample composition. The purpose is then to build a stack of interferometric images (corresponding at each specific position of the sample along Z) by simultaneously moving the sample with the piezoelectric device and recording the resulting image (Fig. 2).
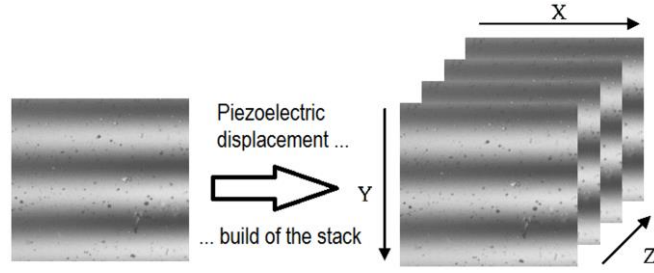
Fig. 2. Interferometric image acquired by the camera and construction of the XYZ image stack.

The interference signal from which the spectral reflectance of the layer is extracted is then obtained by looking at the intensity profile at one specific point of the stack. Because the interference fringes are extracted from 3 x 3 pixel binning in the image stack, the local measurement of the thickness and refractive index is very well spatially resolved: the analysis is made on an area equal to the surface of the diffraction spot in our case. The whole post-processing, from the extraction of the fringes to the application of the fast Fourier transform algorithm and the spectral reflectance obtaining, is detailed in [12,13]. The important point to note is that a calibration step is required in order to extract the spectral reflectance given in Eq. 1. Indeed, the spectrum obtained with this interferometric technique is necessarily proportional to the spectral transfer function (STF), i.e. the spectral signature of the system (light distribution, optical components transmittance, camera spectral response). This calibration step then consists in determining the STF for the given experimental / surrounding conditions of the measurement. Once the STF has been measured, the experimental reflectance spectrum is obtained using the following relation:

$$y_{data}(\lambda) = \left| \frac{FT\left[I(z)\right]}{STF(\lambda)} \right|^2 \quad\quad (2)$$

with $I(z)$ the interferometric signal of the transparent layer as a function of the depth z, FT the Fourier transform operator and y_{data} the experimental reflectance spectrum.

3.2. Processing procedure

Afterwards, the purpose will be to find out the best values of both the thickness and the refractive index enabling the optimization of the fit between the model and the experimental measurement. To assess whether the model fitting is optimized, an error function χ, defined as the quadratic error between the model and the experimental data (Eq. 2), is used. The unknowns, that are the thickness e and refractive index n, are determined so as to minimize the error function as follows:

$$\min_{e,n} \chi(\lambda) = \min_{e,n} \sum_{\lambda \in S} \left[\left| R_{\mathrm{mod}}(\lambda; e, n) \right| - y_{data}(\lambda) \right]^2 \tag{3}$$

with S the spectrum of the white light source. As with the phase of the interferometric signal Fourier transform [4][4][3][3][3], the magnitude also turns out to be highly nonlinear with respect to the unknowns. This necessarily involves the use of a multidimensional nonlinear algorithm to quickly converge towards the best solution. Since the Levenberg-Marquardt nonlinear least-squares algorithm, which is available in MATLAB software, appears to be the most used technique for studying thin film properties, we chose the same algorithm for the present study.

Many studies have shown that this algorithm cannot immediately provide the global minimum of χ since there may exist multiple local minima [4]. The algorithm provides one of them depending on the initial value of the fitting parameters. Some studies were intended to find a good initial estimation of these parameters for quickly converging towards the global minimum [14,15]. In this work, we use an alternative solution which consists in varying the initial values of the pair of parameters (e and n) within one given

range and then recording both the local minimum and the final error (difference between the optimized model and the data) provided by the algorithm. The iteration that leads to the lowest error then corresponds to the global minimum. Despite a slightly longer computing time, this method has proved to be robust and its processing time can be even further shortened if the order of magnitude of these parameters is approximately known, enabling a reduction in the domain of variation of the initial values.

4. Results and discussions

4.1. PMMA layer

To test this spectral method on thick non-absorbing layers, we studied a transparent layer of PMMA (Polymethyl methacrylate) deposited on a substrate of silicon. This material was chosen since its optical properties are very well known, enabling a quick check and validation of the quality of the results. Due to the properties of the polymer and the spin coating deposition method, the layer is quite inhomogeneous, leading to a variation in thickness from 2.5 µm to 4 µm over the field of view. The thickness of the deposited layer was found to be on average 3.33 µm (3.33 ± 0.03 µm) in the area of the measurement using a mechanical profilometer (Dektak stylus).

While the thickness e is only present in the terms of the cosine function (Eq. 1) and will thereby only impact the frequency of the cosine, it is obvious that the index n will affect not only the frequency of the spectrum but also the amplitude of the oscillations since the Fresnel coefficient depends on the refractive index of the layer. To determine both parameters accurately, great care must therefore be taken during the data acquisition process. We previously demonstrated that the numerical aperture (NA) of the objectives could significantly modify the amplitude of the reflectance spectrum reconstructed from

a FT of the fringes [16]. By keeping the NA fully open during the image stack acquisition, errors are induced in the amplitude of the spectrum and we then show that the determination of the refractive index is wrong, subsequently distorting the measurement of the thickness (Fig. 3). Values of 2.292 µm and 2.145 are respectively obtained for the thickness and the refractive index. We recall that the average refractive index of the PMMA is 1.485 in the spectral range studied. By reiterating the acquisition of the PMMA transparent layer with the aperture diaphragm closed, we prevent the amplitude loss of the spectrum and then avoid the error in the measurement of the refractive index (Fig. 4). In this case, the measurement of the thickness is completely consistent with the expected result of ~ 3.33 µm. For this first result, the refractive index was assumed to be constant in the model to speed up the algorithm.
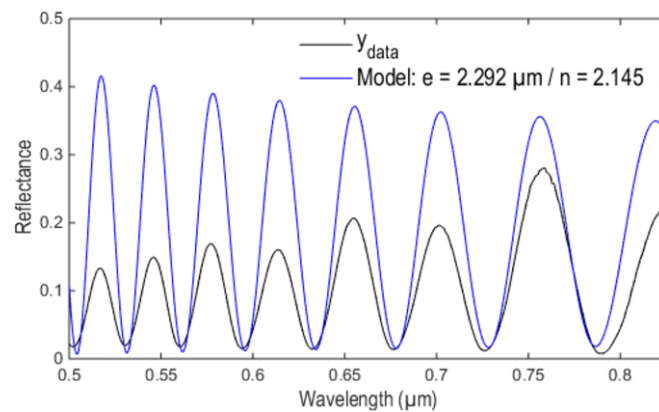
Fig. 3. Comparison between the experimental reflectance spectrum (black curve) and the theoretical optimized model (blue curve) for an illumination aperture of 0.85 (aperture diaphragm fully open).
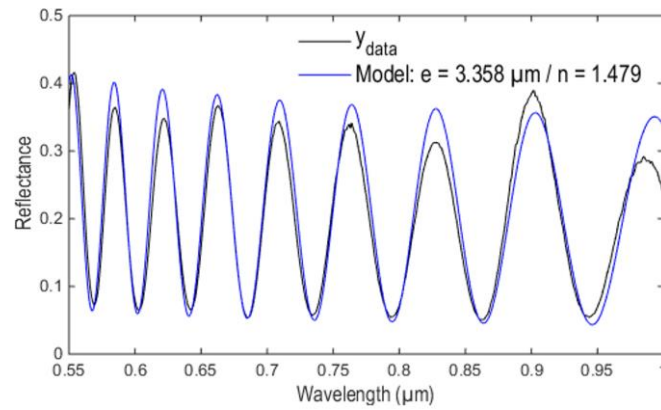
Fig. 4. Comparison between the experimental reflectance spectrum (black curve) and the theoretical optimized model (blue curve) for an illumination aperture of ~ 0.1 (aperture diaphragm closed).

Usually spread over an area of 0.79 μm^2, the diffraction spot becomes more extended (2.27 μm^2) because of the necessity of reducing the system NA, resulting in a lateral resolution that decreases from 0.5 μm to 0.85 μm [16].

It is important to notice that in the work reported in the literature on the thickness measurement of very thin films using this spectral method, no precautions regarding the system NA have been considered. In this particular case, the extremely low thickness of the layer is not sufficient for significantly degrading the interferometric signal, resulting in no need to take this effect into account.

Although the PMMA has a very low dispersion, allowing us at first to consider its refractive index as being constant, we tried to determine its dispersion law. The principle of the processing is the same as that described above, except that the index is now wavelength-dependent. In the reflectance spectrum model, the refractive index is given using either the Cauchy or Sellmeier's law (Eq. 4), usually used to describe the relationship between the optical index and the wavelength within a transparent medium.

$$n_{Cauchy}(\lambda) = A + \frac{B}{\lambda^2}; \qquad n_{Sellmeier}^2(\lambda) = 1 + \frac{B_1\lambda^2}{\lambda^2 - C_1} \tag{4}$$

The index now being a function of two parameters (A and B or B_1 and C_1), this results in

a great increase in the processing time. Indeed, the more parameters that are added to

the model, the longer is the processing time. In order not to increase the computing time

too much, we follow the procedure described below. The first step is identical to the

previous result, consisting in determining both the thickness and the refractive index by

assuming the latter as being constant. This step is quite fast (~ 5 s) and gives us a

precise estimation of e as well as the mean value of n. Thereby, it is subsequently

possible to strongly restrict the range of variation of e. This means that only a few initial

values of e will be tested by the algorithm. In the second step, the optimization

algorithm is inserted into a "while" loop and is focused on testing different combinations

of initial values of the fitting parameters (thickness and those describing the dispersion).

On the first iteration of the loop, the initial values of the dispersion constants are chosen

from a very wide interval since these can have quite different values depending on the

dispersive nature of the layer. The global minimum of χ and the associated error are

extracted from all the local minima provided by the algorithm. At each loop iteration, the

width of the intervals corresponding to the dispersion constants' initial values decreases

by half and become centered on the optimized value of the parameter obtained on the

previous iteration. Then we record the resulting error between the model and the data.

Once the iteration enabling the difference between the errors of the i-th and (i+1)-th steps

to be less than 10^{-6} is reached, the loop is stopped and we consider that the values

provided by the algorithm are optimized. This step-by-step approach makes it possible

to test more values while maintaining a relatively short computation time as well as

increasing the accuracy in the determination of the fitting parameters. The results

obtained from this method and the associated computing times are summarized in Table 1. This analysis has been performed using the parallel pool tool provided by Matlab and enables a time saving of a factor of 3.5. The small differences observed in the values of the thickness and the dispersion constants in function of the zone investigated are caused by the noise present in the processed interferometric signal. The noise being randomly distributed over the field of view, it generates very small disparities in the amplitude of each calculated spectrum and then in the determination of the refractive index. As a result, the thickness measured will also change very slightly. Concerning the thickness measurements, the values obtained vary between 3.3 and 3.36 µm leading to a relative error of less than 1 percent.

Table 1. Measurements of the PMMA layer thickness, dispersion constants and refractive index (at 800 nm) from 5 different regions. The data are compared to the thickness and refractive index (at 800 nm) respectively equal to 3.33 ± 0.03 µm and 1.484 and obtained from a mechanical profilometer (Dektak) and from the literature [17].

Zone	Cauchy's law				Sellmeier's law				Computing time (s)
	e (µm)	A	B	n	e (µm)	B1	C1	n	
1	3.350	1.4768	0.00342	1.482	3.350	1.1811	0.00830	1.482	42.92
2	3.328	1.4757	0.00412	1.482	3.328	1.1782	0.00995	1.482	39.46
3	3.334	1.4815	0.00385	1.488	3.334	1.1952	0.00922	1.487	36.76
4	3.296	1.4820	0.00637	1.492	3.296	1.1973	0.01494	1.492	42.94
5	3.358	1.4725	0.00390	1.479	3.358	1.1686	0.00949	1.479	45.24

The results in Fig. 5 show the refractive index of the PMMA as a function of the wavelength calculated from Eq. 4 using the values of the constants of the zones 2 and 3. In each case, both the Cauchy's and Sellmeier's laws are plotted and are superimposed. As reference results, we used the data extracted from the literature [17] (dotted line), [18] (full line), [19] (dashed line). On Fig. 6, the average refractive index and the

standard deviation from the 5 measurement points are plotted and are compared to the dispersion law of the PMMA found in the literature. This comparison shows an almost perfect match with our local measurements and demonstrates the good performance of the proposed technique for such samples.
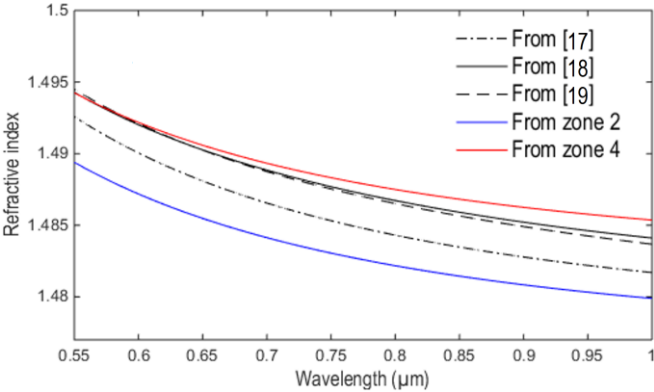

Fig. 5. Dispersion of the PMMA. The three black curves are obtained from the literature and are used as reference. The blue and red curves are respectively obtained from the zones 2 and 3.
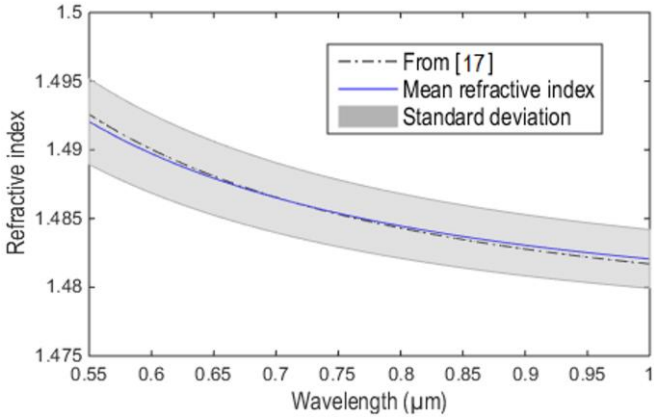

Fig. 6. Dispersion law of the PMMA in the [550 nm, 1000 nm] wavelength range. The average refractive index as well as the standard deviation from the five measurements are plotted and compared to the data found in the literature [17].

4.2. SnO2 layer

In order to test the local characterization technique on a more complicated sample, we studied a layer of tin oxide. Indeed, the dispersion of the SnO_2 is much stronger than that of the PMMA in the studied spectral range. The SnO_2 film has been deposited onto silicon substrate at 100°C using a tin target in the reactive magnetron sputtering system AJA ORION 3.

As explained previously, the acquisition of this sample has been carried out with the aperture diaphragm closed as much as possible to prevent any loss in the amplitude of the reflectance spectrum. The SnO_2 layer has been measured at 10 different points and the results are summarized in Table 2. For each zone, we compare the values of both the thickness and the refractive index given by the algorithm for two models. The first model assumes the refractive index as a constant while in the model 2, the index is expressed using the Sellmeier's law. As demonstrated on Fig. 7, by taking a wavelength-dependent index, the match between the experimental spectrum (black curve) and the model (blue curve) is more pronounced, resulting in a determination of the thickness and refractive index more accurate.
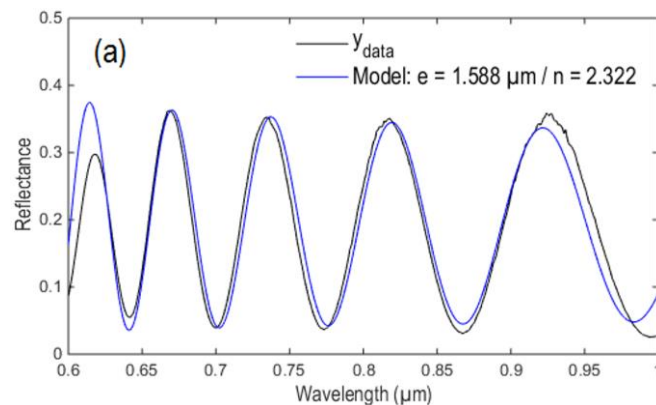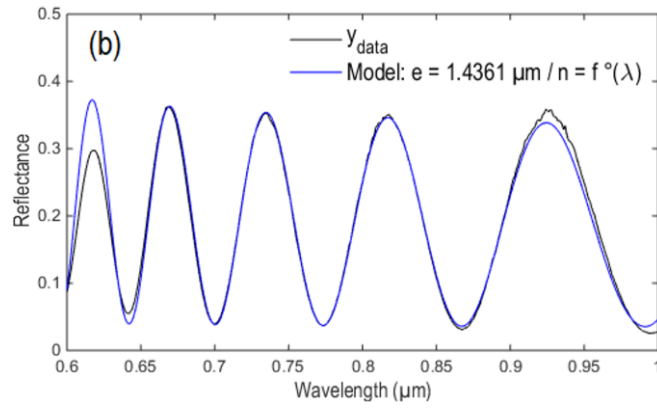
Fig. 7. Comparison between the experimental reflectance spectrum (black curve) and the theoretical optimized model (blue curve). (a) n is constant (Model 1). (b) n is function of the wavelength (Model 2).

As reference values, we used the data provided by other techniques. The thickness was measured using the Dektak mechanical profilometer and was found to be 1.422 ± 0.03 µm. For the refractive index, a Jobin-Yvon ellipsometer has been used but did not lead to usable results due to the excessive thickness of the layer resulting in too fine oscillations that could not be resolved. Consequently, another sample with a thickness of less than 100 nm was manufactured and used for ellipsometric measurements. The refractive index data vary from 2.37 up to 2.24 in the wavelength range of [600 nm ; 1000 nm].

Table 2. Measurements of the SnO$_2$ layer thickness and refractive index from 10 different regions. The data are compared to the thickness and refractive index (at 800 nm) respectively equal to 1.422 ± 0.03 µm and 2.279 and obtained from a mechanical profilometer (Dektak) and from an ellipsometer.

Zone	Model 1: n is constant		Model 2: Sellmeier's law		Computing time (s)
	e (µm)	n	e (µm)	n (at 800 nm)	
1	1.572	2.349	1.424	2.305	13.31
2	1.572	2.349	1.422	2.309	13.35
3	1.580	2.337	1.434	2.288	15.54
4	1.580	2.333	1.427	2.295	14.04
5	1.588	2.322	1.436	2.281	13.32
6	1.576	2.343	1.429	2.298	13.90
7	1.585	2.330	1.437	2.284	15.70

8	1.572	2.344	1.420	2.308	11.55
9	1.575	2.338	1.425	2.299	11.68
10	1.572	2.348	1.422	2.308	18.34

It is worth noting that when the refractive index is assumed to be constant, the thickness provided by the algorithm is quite far from the expected value of 1.422 µm. However, with the model 2, all the thickness values are well consistent and are included in the uncertainty area of the mechanical measurement as shown in Fig. 8. This demonstrates the need to use a wavelength-dependent parameter to avoid errors in the determination of the thickness of rather dispersive samples.
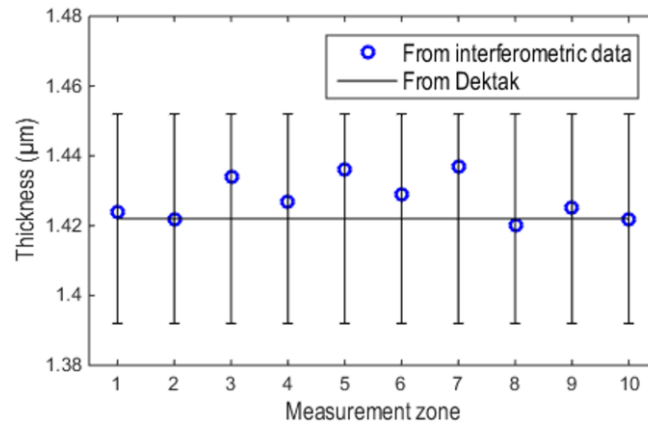
Fig. 8. Thickness of the SnO₂ layer over the 10 measurement areas. The blue circles represent the measurements performed using the presented technique. The black lines are the values obtained from the Dektak and the associated uncertainty.

Using the values of the dispersion constants provided by the algorithm and then by applying Eq. 4, we plotted the average refractive index and the standard deviation from the 10 measurements. The dispersion law of the SnO₂ layer is compared to that obtained with the ellipsometer.
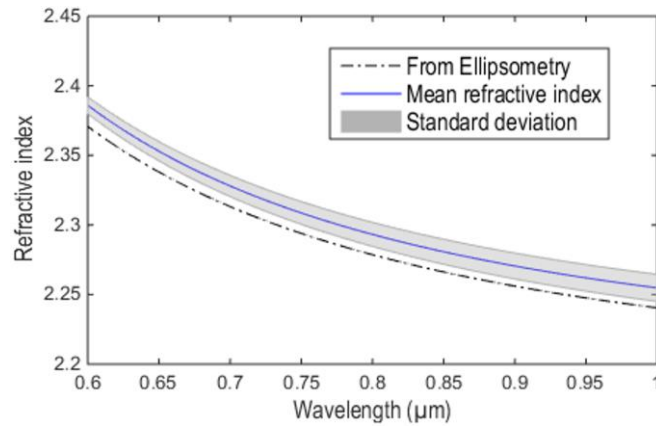
Fig. 9. Dispersion law of the SnO$_2$ in the [600 nm, 1000 nm] wavelength range. The average refractive index as well as the standard deviation from the ten measurements are plotted and compared to the ellipsometric data.

Compared to the results obtained on the PMMA layer, it can be noticed that the reference curve of the refractive index is not included in the margin of error of the experimental measurements. This can be explained by the fact that the ellipsometric measurement was not performed on the sample studied. We used another sample, perhaps manufactured under slightly different conditions, which can explain the little difference between the curves. Nevertheless, it is important to underline that the trend of the refractive index curve, representing the dispersion of the layer, is well recovered.

As mentioned previously, the accuracy of the measurements is related to the level of noise present in the processed interference signal and could significantly degrade the quality of the characterizations in more complex samples like absorbing or scattering media where the signal to noise ratio is much lower. The study of such samples is a part of our future work.

5. Conclusion

In conclusion, we have presented an improved interferometric method, extended from that normally used for very thin films, to locally investigate the optical and morphological properties of thick transparent layers having a thickness exceeding the coherence length of the illumination source. This approach can be used for probing both the thickness and the optical index (as a function of the wavelength) of a transparent layer at a specific point. By reiterating the local process in the three directions of space, this approach could be used for providing a full data volume of both the thickness and the index with a spatial resolution better than 1 μm. It has been shown that this technique can be used for characterizing dispersive samples, but, contrary to what happens with very weakly dispersive layers, considering a wavelength-dependent index during the optimization process is essential. For now limited to transparent layers, further work would be to extend the applications to more complicated samples.

References:

[1] P. Montgomery, D. Montaner, O. Manzardo, M. Flury, H. Herzig, The metrology of a miniature FT spectrometer MOEMS device using white light scanning interference microscopy, Thin Solid Films. 450 (2004) 79–83.

[2]   E. Halter, P. Montgomery, D. Montaner, R. Barillon, M. Del Nero, C. Galindo, S. Georg, Characterization of inhomogeneous colloidal layers using adapted coherence probe microscopy, Appl. Surf. Sci. 256 (2010) 6144–6152. doi:10.1016/j.apsusc.2010.02.019.

[3]   P.C. Montgomery, D. Montaner, F. Salzenstein, Tomographic analysis of medium thickness transparent layers using white light scanning interferometry and XZ fringe image processing, in: SPIE Photonics Eur., International Society for Optics and Photonics, 2012: pp. 843014-843014–9. doi:10.1117/12.927813.

[4]   S.-W. Kim, G.-H. Kim, Thickness-profile measurement of transparent thin-film layers by white-light scanning interferometry, Appl. Opt. 38 (1999) 5968–5973.

[5]   S.K. Debnath, M.P. Kothiyal, J. Schmit, P. Hariharan, Spectrally resolved white-light phase-shifting interference microscopy for thickness-profile measurements of transparent thin film layers on patterned substrates, Opt. Express. 14 (2006) 4662–4667. doi:10.1364/OE.14.004662.

[6]   D.-S. Wan, Measurements of thin films using fourier amplitude, US 7612891 B2, 2009.

[7]   J. Dong, R. Lu, Sensitivity analysis of thin-film thickness measurement by vertical scanning white-light interferometry, Appl. Opt. 51 (2012) 5668–5675. doi:10.1364/AO.51.005668.

[8]   M.-C. Li, D.-S. Wan, C.-C. Lee, Application of white-light scanning interferometer on transparent thin-film measurement, Appl. Opt. 51 (2012) 8579–8586. doi:10.1364/AO.51.008579.

[9]   M. Born, E. Wolf, Principles of Optics: Electromagnetic Theory of Propagation, Interference and Diffraction of Light, Elsevier, 2013.

[10] A. Federici, H.S. Gutierrez da Costa, J. Ogien, A.K. Ellerbee, A. Dubois, Wide-field, full-field optical coherence microscopy for high-axial-resolution phase and amplitude imaging, Appl. Opt. 54 (2015) 8212. doi:10.1364/AO.54.008212.

[11] M.A. Green, Self-consistent optical parameters of intrinsic silicon at 300K including temperature coefficients, Sol. Energy Mater. Sol. Cells. 92 (2008) 1305–1310. doi:10.1016/j.solmat.2008.06.009.

[12] R. Claveau, P.C. Montgomery, M. Flury, D. Montaner, Local reflectance spectra measurements of surfaces using coherence scanning interferometry, in: SPIE Photonics Eur., International Society for Optics and Photonics, 2016: p. 98900Q–98900Q–12. doi:10.1117/12.2227625.

[13] R. Claveau, P.C. Montgomery, M. Flury, Spatially-Resolved Spectroscopic Characterization of Reflective and Transparent Materials at a Micro-Meter Scale Using Coherence Scanning Interferometry, Phys. Status Solidi C. 14 (2017) 1700157. doi:10.1002/pssc.201700157.

[14] T. Guo, J. Wu, L. Ni, X. Fu, X. Hu, Initial estimation of thin film thickness measurement based on white light spectral interferometry, Thin Solid Films. 612 (2016) 267–273. doi:10.1016/j.tsf.2016.06.025.

[15] T. Jo, K. Kim, S. Kim, H. Pahk, Thickness and Surface Measurement of Transparent Thin-Film Layers using White Light Scanning Interferometry Combined with Reflectometry, J. Opt. Soc. Korea. 18 (2014) 236–243. doi:10.3807/JOSK.2014.18.3.236.

[16] R. Claveau, P. Montgomery, M. Flury, D. Montaner, Depth-resolved local reflectance spectra measurements in full-field optical coherence tomography, Opt. Express. 25 (2017) 20216–20232. doi:10.1364/OE.25.020216.

[17] N. Sultanova, S. Kasarova, I. Nikolov, Dispersion Proper ties of Optical Polymers, Acta Phys. Pol.-Ser. Gen. Phys. 116 (2009) 585.

[18] G. Beadie, M. Brindza, R.A. Flynn, A. Rosenberg, J.S. Shirk, Refractive index measurements of poly(methyl methacrylate) (PMMA) from 04–16 µm, Appl. Opt. 54 (2015) F139. doi:10.1364/AO.54.00F139.

[19] T. Ishigure, E. Nihei, Y. Koike, Optimum refractive-index profile of the graded-index polymer optical fiber, toward gigabit data links, Appl. Opt. 35 (1996) 2048–2053.

Fig. 8. Thickness of the SnO$_2$ layer over the 10 measurement areas. The blue circles represent the measurements performed using the presented technique. The black lines are the values obtained from the Dektak and the associated uncertainty.

Fig. 9. Dispersion law of the SnO$_2$ in the [600 nm, 1000 nm] wavelength range. The average refractive index as well as the standard deviation from the ten measurements are plotted and compared to the ellipsometric data.

Table 1. Measurements of the PMMA layer thickness, dispersion constants and refractive index (at 800 nm) from 5 different regions. The data are compared to the thickness and refractive index (at 800 nm) respectively equal to 3.33 μm and 1.484 and obtained from a mechanical profilometer (Dektak) and from the literature [17].

Table 2. Measurements of the SnO$_2$ layer thickness and refractive index from 10 different regions. The data are compared to the thickness and refractive index (at 800 nm) respectively equal to 1.422 ± 0.03 μm and 2.279 and obtained from a mechanical profilometer (Dektak) and from an ellipsometer.